SCIENCE CHINA
Information Sciences

• **Supplementary File** •

Manifold optimization assisted centralized hybrid precoding for cell-free massive MIMO systems

Jie LUO[1], Jiancun FAN[1,2*], Yawen WANG[1] & Jinbo ZHANG[2]

[1]*School of Information and Communications Engineering, Xi'an Jiaotong University, Xi'an* 710049*, China;*
[2]*Science and Technology on Communication Networks Laboratory, Shijiazhuang* 50081*, China*

Appendix A The scalability gained by dynamic cooperation

In practical applications, not all APs need to serve all users, and the connection between them depends on channel conditions, as shown in Fig. A1. Due to the large path loss of mmWaves, the access decision condition is generally based on distance. Therefore, we can define a connection matrix $\mathbf{C} \in \mathcal{R}^{M\times K}$ to represent the selective access between APs and users,

$$\mathbf{C}_{m,k} = \begin{cases} 0, & \text{if } \|\mathbf{H}_{m,k}\|_2 < a \\ 1, & \text{if } \|\mathbf{H}_{m,k}\|_2 \geqslant a \end{cases}, \tag{A1}$$

where a is the threshold value, depending on the deployment environment. In this way, the set of users served by the mth AP can be expressed as $\Upsilon_m = \{k : \mathbf{C}_{m,k} = 1, k \in \{1,\ldots,K\}\}$, and the set of APs serving the kth user is $\Omega_k = \{m : \mathbf{C}_{m,k} = 1, m \in \{1,\ldots,M\}\}$.

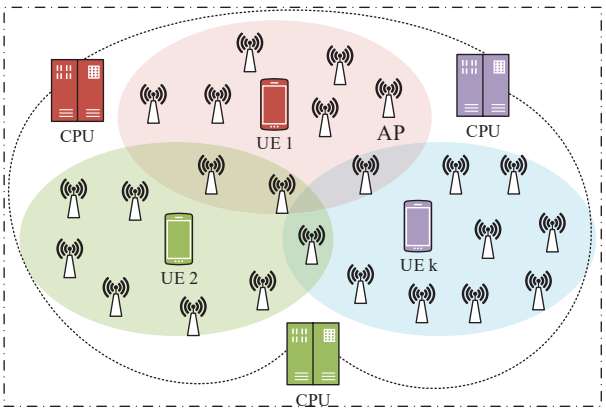

Figure A1 Dynamic cooperation in the scalable cell-free massive MIMO system.

Note that, since the focus of this letter is not on the user selection problem, we only adopt a simple model, as shown in equation (A1), to illustrate the scalability of the user-centric cell-free system. In fact, the user selection problem is very complicated because the AP can support a limited number of users, and the selection of users has been widely studied in scalable cell-free MIMO systems [1, 2].

To unify with the received signal model, we also define a series of diagonal matrices $\mathbf{D}_k = \text{blkdiag}\left(\mathbf{D}_{1,k},\ldots,\mathbf{D}_{M,k}\right)$ to construct the equivalent channel $\hat{\mathbf{H}}_k^{\mathrm{H}} = \mathbf{H}_k^{\mathrm{H}}\mathbf{D}_k$ for $k = 1,\ldots,K$, where $\mathbf{D}_{m,k} \in \mathbb{C}^{N\times N}$,

$$\mathbf{D}_{m,k} = \begin{cases} \mathbf{I}_N, & \text{if } \mathbf{C}_{m,k} = 1 \\ \mathbf{0}_N, & \text{if } \mathbf{C}_{m,k} = 0 \end{cases}. \tag{A2}$$

Appendix B Fully-digital precoding design

In this section, the hybrid precoding matrix composed of analog and digital precoders $(\mathbf{F}^{\mathrm{RF}}, \mathbf{F}_k^{\mathrm{DD}})$ is regarded as a whole $\mathbf{F}_k = \mathbf{F}^{\mathrm{RF}}\mathbf{F}_k^{\mathrm{DD}}$, and the internal non-convex constraints are not considered, thus the process of solving $\mathbf{F}_k$ is simplified. We solve the fully-digital precoder $\mathbf{F}_k$ from two different perspectives: IC and WS-MMSE criteria.

* Corresponding author (email: fanjc0114@gmail.com)

Appendix B.1 IC criteria

We propose an improved block-diagonal fully-digital precoding scheme based on subspace decomposition to eliminate inter-user interference. By designing $\mathbf{F}_k$ at each AP to satisfy $\hat{\mathbf{H}}_k^{\mathrm{H}}\tilde{\mathbf{F}}_k\tilde{\mathbf{s}}_k = 0$, where

$$\tilde{\mathbf{F}}_k = [\mathbf{F}_1, \ldots, \mathbf{F}_{k-1}, \mathbf{F}_{k+1}, \cdots, \mathbf{F}_K], \tag{B1a}$$

$$\tilde{\mathbf{s}}_k = [s_1, \ldots, s_{k-1}, s_{k+1}, \ldots s_K]^T \in \mathbb{C}^{(K-1)\times 1}. \tag{B1b}$$

It is equivalent to $\hat{\mathbf{H}}_k^{\mathrm{H}}\mathbf{F}_i = 0, i \neq k$, and it means that the interference between users is zero. The corresponding optimization problem can be expressed as

$$\mathbf{F} \triangleq [\mathbf{F}_1, \ldots, \mathbf{F}_K] = \underset{tr(\mathbf{F}_k\mathbf{F}_k^{\mathrm{H}})\leqslant 1}{\arg} \hat{\mathbf{H}}_k^{\mathrm{H}}\tilde{\mathbf{F}}_k\tilde{\mathbf{s}}_k = 0. \tag{B2}$$

We first define $\tilde{\mathbf{H}}_k^{\mathrm{H}} = \left[\hat{\mathbf{H}}_1, \ldots, \hat{\mathbf{H}}_{k-1}, \hat{\mathbf{H}}_{k+1}, \ldots, \hat{\mathbf{H}}_K\right]^{\mathrm{H}}$. Through the matrix subspace analysis, it can be known that $\mathbf{F}_k$ must fall in the null space of $\tilde{\mathbf{H}}_k^{\mathrm{H}}$, so only when the dimension of the null space of $\tilde{\mathbf{H}}_k^{\mathrm{H}}$ is greater than 0, the signal may be sent to user k, that is, it needs to satisfy rank $\left(\tilde{\mathbf{H}}_k^{\mathrm{H}}\right) < MN$. Since $MN > K-1$, rank $\left(\tilde{\mathbf{H}}_k^{\mathrm{H}}\right) \leqslant \min(MN, K-1) < MN$ obviously holds.

Let $\tilde{\mathrm{r}}_k$= rank $\left(\tilde{\mathbf{H}}_k^{\mathrm{H}}\right) \leqslant K-1$, then the *singular value decomposition* (SVD) of $\tilde{\mathbf{H}}_k^{\mathrm{H}}$ is

$$\tilde{\mathbf{H}}_k^{\mathrm{H}} = \tilde{\mathbf{U}}_k\tilde{\mathbf{\Sigma}}_k\left[\tilde{\mathbf{V}}_k^{(1)}\tilde{\mathbf{V}}_k^{(0)}\right]^{\mathrm{H}}, \tag{B3}$$

where $\tilde{\mathbf{V}}_k^{(1)}$ contains the first $\tilde{\mathrm{r}}_k$ right singular value vectors, and $\tilde{\mathbf{V}}_k^{(0)}$ contains the last $MN - \tilde{\mathrm{r}}_k$ right singular value vectors. According to matrix theory, the columns of $\tilde{\mathbf{V}}_k^{(0)}$ compose the precoding matrix $\mathbf{F}_k$ of the kth user. In this case, the joint equivalent channel can be expressed as

$$\hat{\mathbf{H}}_{eq}^{\mathrm{H}} = \begin{bmatrix} \hat{\mathbf{H}}_1^{\mathrm{H}}\tilde{\mathbf{V}}_1^{(0)} & \cdots & 0 \\ \vdots & \ddots & \vdots \\ 0 & \cdots & \hat{\mathbf{H}}_K^{\mathrm{H}}\tilde{\mathbf{V}}_K^{(0)} \end{bmatrix}. \tag{B4}$$

The SVD of diagonal element $\hat{\mathbf{H}}_k^{\mathrm{H}}\tilde{\mathbf{V}}_k^{(0)}$ is

$$\hat{\mathbf{H}}_k^{\mathrm{H}}\tilde{\mathbf{V}}_k^{(0)} = \mathbf{U}_k\begin{bmatrix} \mathbf{\Sigma}_k & 0 \\ 0 & 0 \end{bmatrix}\left[\mathbf{V}_k^{(1)}\mathbf{V}_k^{(0)}\right]^{\mathrm{H}}, \tag{B5}$$

where $\mathbf{\Sigma}_k$ is a $\hat{\mathrm{r}}_k \times \hat{\mathrm{r}}_k$ dimensional matrix, then $\mathbf{F}_k = \tilde{\mathbf{V}}_k^{(0)}\mathbf{V}_k^{(1)}$, and the water-filling algorithm is used for power distribution, and we can get

$$\mathbf{F}^{\mathrm{IC}} \triangleq \left[\tilde{\mathbf{V}}_1^{(0)}\mathbf{V}_1^{(1)}, \ldots, \tilde{\mathbf{V}}_K^{(0)}\mathbf{V}_K^{(1)}\right]\Lambda^{1/2}, \tag{B6}$$

where $\Lambda = \mathrm{diag}(\lambda_1, \ldots, \lambda_K)$ is the result of the water-filling algorithm.

Appendix B.2 WS-MMSE criteria

In [3], the maximizing achievable rate problem can be approximately equivalently transformed into an MMSE problem. In this letter, MSE is denoted as

$$\mathrm{E}_k = \mathbb{E}\left[(y_k - s_k)(y_k - s_k)^H\right] = \sum_{i\in\mathcal{K}}\hat{\mathbf{H}}_k^{\mathrm{H}}\mathbf{F}_i\mathbf{F}_i^{\mathrm{H}}\hat{\mathbf{H}}_k - \hat{\mathbf{H}}_k^{\mathrm{H}}\mathbf{F}_k - \mathbf{F}_k^{\mathrm{H}}\hat{\mathbf{H}}_k + \sigma_k^2 + 1, \tag{B7}$$

then WS-MSE can be denoted as

$$\sum_{k\in\mathcal{K}}\omega_k\mathrm{E}_k = \mathrm{tr}\left(\mathbf{F}^{\mathrm{H}}\mathbf{\Phi}\mathbf{F}\right) - 2\mathrm{Re}\left[\mathrm{tr}\left(\mathbf{\Omega}\hat{\mathbf{H}}^{\mathrm{H}}\mathbf{F}\right)\right] + \sum_{k\in\mathcal{K}}\omega_k\left(\sigma_k^2 + 1\right), \tag{B8}$$

where $\mathrm{Re}(\cdot)$ denotes the real part of a complex variable, $\mathbf{\Omega} = \mathrm{diag}(\omega_1, \ldots, \omega_K)$, and

$$\mathbf{\Phi} = \begin{bmatrix} \mathbf{\Phi}_{11} & \cdots & \mathbf{\Phi}_{1M} \\ \vdots & \ddots & \vdots \\ \mathbf{\Phi}_{1M}^{\mathrm{H}} & \cdots & \mathbf{\Phi}_{MM} \end{bmatrix} \tag{B9}$$

with $\mathbf{\Phi}_{ij} = \sum_{k\in\mathcal{K}}\omega_k\hat{\mathbf{H}}_{i,k}\hat{\mathbf{H}}_{j,k}^{\mathrm{H}} \in \mathbb{C}^{N\times 1}$. The corresponding optimization problem can be expressed as

$$\min_{\mathbf{F}_k} \quad \mathrm{tr}\left(\mathbf{F}^{\mathrm{H}}\mathbf{\Phi}\mathbf{F}\right) - 2\mathrm{Re}\left[\mathrm{tr}\left(\mathbf{\Omega}\hat{\mathbf{H}}^{\mathrm{H}}\mathbf{F}\right)\right] \tag{B10a}$$

$$\text{s.t.} \quad \|\mathbf{F}_k\|_{\mathrm{F}}^2 \leqslant 1, \forall k \tag{B10b}$$

$$\sum_{k=1}^{K}\|\mathbf{F}_{m,k}\|^2 \leqslant \rho_{\mathrm{AP}}, \forall m. \tag{B10c}$$

In the process of solving problem (B10), the condition (B10b) can be ignored first, and it only needs to be normalized in the final output. For the kth user, the *Karush-Kuhn-Tucker* (KKT) condition of (B10) is

$$\nabla_{\mathbf{F}_k}\left(\sum_{k\in\mathcal{K}}\omega_k \mathrm{E}_k+\sum_{m\in\mathcal{AP}}\lambda_m\left(\sum_{k\in\mathcal{K}}\left\|\mathbf{F}_{m,k}\right\|^2-\rho_{\mathrm{AP}}\right)\right)=\mathbf{0}, \tag{B11}$$

where λ_m is the dual variable related to ρ_{AP}. By solving (B11), we can get the fully-digital precoder based on the WS-MMSE criterion.

$$\mathbf{F}_k^{\mathrm{WS-MMSE}}=\omega_k\left(\mathbf{\Phi}+\sum_{m\in\mathcal{AP}}\lambda_m\mathbf{I}_N\right)^{-1}\hat{\mathbf{H}}_k. \tag{B12}$$

Appendix C Riemann gradient

To remove non-convex constraints of anolog precoder such as block diagonalization constraint and unit modulus constraint, we transform the optimization space from Euclidean space to Riemann space and define the Riemann gradient. From duality theory [4], we know that solving optimization problems on Riemannian manifolds is locally similar to optimization on Euclidean spaces with smooth constraints.

Algorithm C1 Manifold optimization for analog precoding

Input: $\mathbf{F}^{\mathrm{IC}}$ or $\mathbf{F}^{\mathrm{WS-MMSE}}$, $\mathbf{F}^{\mathrm{DD}}$, $\mathbf{x}_0\in\mathcal{M}_{circle}^V$
1: Initialization: $\mathbf{h}_0=-\operatorname{grad}f(\mathbf{x}_0)$, and $t=0$;
2: **repeat**
3: Choose line search step size α_t;
4: Find the next point $\mathbf{x}_{t+1}$ with (C7);
5: Calculate the Riemann gradient $\mathbf{g}_{t+1}$ with (C5);
6: Calculate the vector transport $\mathbf{h}_t^+$ of $\mathbf{h}_t$ from $\mathbf{x}_t$ to $\mathbf{x}_{t+1}$ with $\mathbf{h}_t^+\mapsto\mathbf{h}_t-\Re\left\{\mathbf{h}_t\circ\mathbf{x}_{t+1}^*\right\}\circ\mathbf{x}_{t+1}$;
7: Choose a Polak-Ribiere parameter β_{t+1};
8: Compute the conjugate direction $\mathbf{h}_{t+1}=-\mathbf{g}_{t+1}+\beta_{t+1}\mathbf{h}_t^+$;
9: $t\leftarrow t+1$;
10: **until** a stopping criterion triggers, such as $\mathbf{g}_{t+1}=0$.

In Riemann space, the unit complex circle can be represented as

$$\mathcal{M}_{circle}=\left\{x\in\mathbb{C}:x^*x=1\right\}. \tag{C1}$$

For a random point $x\in\mathcal{M}_{circle}$, its tangent space at point x is

$$T_x\mathcal{M}_{circle}=\left\{y\in\mathbb{C}:x^*y+y^*x=2\left\langle x,y\right\rangle=0\right\}, \tag{C2}$$

where $\langle x_1,x_2\rangle=\Re\left\{x_1^*x_2\right\}$ is the Riemann inner product and $\Re(\cdot)$ represents the real part of a complex variable.

In order to facilitate optimization, the analog precoding matrix is vectorized, that is, $\mathbf{x}=\mathrm{vec}\left(\mathbf{F}^{\mathrm{RF}}\right)$, so that the non-convex property of diagonalization can be ignored when using manifold optimization. Due to its block-diagonalized characteristics, we only take the elements on the diagonal, and the length of $\mathbf{x}$ is $V=MNN_{\mathrm{RF}}$. Besides, considering the existence of the unit modulus constraint, $\mathbf{x}$ can also be regarded as a high-order complex circular manifold.

$$\mathcal{M}_{circle}^V=\left\{\mathbf{x}\in\mathbb{C}^V:x_1^*x_1=x_2^*x_2=\cdots=x_V^*x_V=1\right\}. \tag{C3}$$

Similarly, the tangent plane of any point on the manifold $\mathcal{M}_{circle}^V$ can be expressed as

$$T_{\mathbf{x}}\mathcal{M}_{circle}^V=\left\{\mathbf{y}\in\mathbb{C}^V:\Re\left\{\mathbf{y}\circ\mathbf{x}^*\right\}=\mathbf{0}_V\right\}. \tag{C4}$$

Similar to Euclidean space, the Riemann gradient at $\mathbf{x}$ can be represented by a tangent vector $\operatorname{grad}f(\mathbf{x})$, which can be obtained by orthogonally projecting the Euclidean gradient $\nabla f(\mathbf{x})$ onto the tangent plane $T_{\mathbf{x}}\mathcal{M}_{circle}^V$ [5].

$$\operatorname{grad}f(\mathbf{x})=\mathrm{Proj}_{\mathbf{x}}\left\{\nabla f(\mathbf{x})\right\}=\nabla f(\mathbf{x})-\mathrm{Re}\left\{\nabla f(\mathbf{x})\circ\mathbf{x}^*\right\}\circ\mathbf{x}, \tag{C5}$$

where the Euclidean gradient of P4 (6a) is

$$\nabla f(\mathbf{x})=-2\left(\left(\mathbf{F}^{\mathrm{DD}}\right)^*\otimes\mathbf{I}_{MN}\right)\left[\mathrm{vec}\left(\mathbf{F}^{\mathrm{IC}}\right)-\left(\left(\mathbf{F}^{\mathrm{DD}}\right)^{\mathrm{T}}\otimes\mathbf{I}_{MN}\right)\mathbf{x}\right], \tag{C6}$$

where $\circ$ and $\otimes$ are the Hadamard and Kronecker product, respectively.

In the process of gradient descent, there is an inevitable over-optimization situation, which requires backtracking correction. At point $\mathbf{x}\in\mathcal{M}_{circle}^V$, the backtracking of tangent vector $\alpha\mathbf{h}$ can be expressed as

$$\mathrm{Back}_{\mathbf{x}}:\ T_{\mathbf{x}}\mathcal{M}_{circle}^V\to\mathcal{M}_{circle}^V:\alpha\mathbf{h}\mapsto\mathrm{Back}_{\mathbf{x}}(\alpha\mathbf{h})=\mathrm{vec}\left[\frac{(\mathbf{x}+\alpha\mathbf{h})_i}{\left|(\mathbf{x}+\alpha\mathbf{h})_i\right|}\right]. \tag{C7}$$

In Algorithm C1, we summarize the steps of the Riemann gradient descent-based manifold optimization algorithm for solving analog precoders, where the Polak-Ribiere parameter [5] is used to ensure that the objective function is non-increasing in each iteration.

Algorithm D1 MO-CHP algorithm

Input: $\mathbf{F}^{\mathrm{IC}}$ or $\mathbf{F}^{\mathrm{WS-MMSE}}$, Algorithm C1

1: Initialization: $\left(\mathbf{F}^{\mathrm{RF}}\right)^{0}$ with random phases and $r=0$;
2: **repeat**
3: Fix $\left(\mathbf{F}^{\mathrm{RF}}\right)^{r}$, and $\left(\mathbf{F}^{\mathrm{DD}}\right)^{r}=\left(\left(\mathbf{F}^{\mathrm{RF}}\right)^{r}\right)^{\dagger}\mathbf{F}^{\mathrm{IC}}$;
4: Optimize $\left(\mathbf{F}^{\mathrm{RF}}\right)^{r+1}$ with Algorithm C1;
5: $r \leftarrow r+1$;
6: **until** $\left\|\mathbf{F}^{\mathrm{IC}}-\left(\mathbf{F}^{\mathrm{RF}}\right)^{r}\left(\mathbf{F}^{\mathrm{DD}}\right)^{r}\right\|_{\mathrm{F}}^{2} \leqslant 0.01$;
7: For the baseband digital precoder, meet the power constraints and normalize $\mathbf{F}_{k}^{\mathrm{DD}}=\frac{\mathbf{F}_{k}^{\mathrm{DD}}}{\left\|\mathbf{F}^{\mathrm{RF}}\mathbf{F}_{k}^{\mathrm{DD}}\right\|_{\mathrm{F}}}$.

Output: $\mathbf{F}^{\mathrm{RF}}$, $\mathbf{F}^{\mathrm{DD}}$

Appendix D Computational complexity

The alternate optimization process based on Riemann manifold is summarized as Algorithm D1. In fact, when we adopt the WS-MMSE method, we only need to replace $\mathbf{F}^{\mathrm{IC}}$ with $\mathbf{F}^{\mathrm{WS-MMSE}}$.

In this section, we analyze the computational complexity of the proposed MO-CHP scheme by the number of complex multiplications. It mainly comes from two parts, one is the process of solving the standard fully-digital precoder, and the other is the process of solving the analog precoder using manifold optimization. To simplify the presentation, we denote the total number of antennas of all APs as $N_{total}=MN$. Since the IC criterion mainly adopts the method of subspace decomposition, its computational complexity can be expressed as $\mathcal{O}_{1}^{\mathrm{IC}}=\mathcal{O}\left\{K\left(N_{total}^{3}+N_{total}\right)\right\}$. Similarly, when the WS-MMSE criterion is used to obtain the fully-digital precoder, its computational complexity is $\mathcal{O}_{1}^{\mathrm{WS-MMSE}}=\mathcal{O}\left\{K\left(N_{total}^{3}+2N_{total}^{2}+N_{total}\right)\right\}$. In manifold optimization, its complexity mainly comes from three subparts: conjugate gradient calculation, orthogonal projection and linear search, which are

$$\mathcal{O}\left(4N_{total}^{2}N_{\mathrm{RF}}K+N_{total}N_{\mathrm{RF}}^{2}K^{2}+N_{\mathrm{RF}}^{3}K^{3}\right), \tag{D1a}$$

$$\mathcal{O}\left(2N_{total}N_{\mathrm{RF}}K+N_{total}\right), \tag{D1b}$$

$$\mathcal{O}\left(N_{total}^{2}N_{\mathrm{RF}}K+2N_{total}N_{\mathrm{RF}}^{2}K^{2}+N_{\mathrm{RF}}^{3}K^{3}\right). \tag{D1c}$$

Generally, the number of RF links of a single AP is $N_{\mathrm{RF}}=1$ to make the AP smaller and easier to deploy. Thus, the complexity of one iteration can be further expressed as

$$\mathcal{O}_{iter}=\mathcal{O}\left(7N_{total}^{2}K+3N_{total}K^{2}+2K^{3}+N_{total}\right). \tag{D2}$$

So that, the total complexity of proposed MO-CHP scheme is $\mathcal{O}_{Total}=\mathcal{O}_{1}+N_{out}N_{in}\mathcal{O}_{iter}$, where N_{out}, N_{in} are the number of outer and inner iterations, respectively.

Appendix E Simulation details

The simulation environment is configured as follows, the AP locations obey a Poisson distribution in the rectangular coverage area with length and width of 2 km and 1 km respectively. In addition, the density of APs is $\lambda_{\mathrm{AP}}=4\mathrm{APs/km}^{2}$, and it serves $K=4$ users on the same frequency at the same time. Taking into account the limited number of scatterers in the mmWave propagation environment, we adopt the classic Saleh-Valenzuela channel model, and $\mathbf{H}_{m,k}$ can be modeled as

$$\mathbf{H}_{m,k}=\sqrt{\frac{N}{L_{m,k}}}\sum_{l=1}^{L_{m,k}}\beta_{m,k}^{(l)}\mathbf{f}\left(\varphi_{m,k}^{(l)}\right), \tag{E1}$$

where $\sqrt{\frac{N}{L_{m,k}}}$ is the power normalization factor, $L_{m,k}$ is the number of paths between mth AP and kth user, $\beta_{m,k}^{(l)}$ and $\varphi_{m,k}^{(l)}$ are the complex gain and *angles of departure* (AoD) of the lth path between mth AP and kth user, respectively. The array response of *uniform linear array* (ULA) with N antennas can be expressed as

$$\mathbf{f}\left(\varphi\right)=\frac{1}{\sqrt{N}}[1,e^{j\frac{2\pi}{\lambda}d\sin(\varphi)},\ldots,e^{j\frac{2\pi}{\lambda}d(N-1)\sin(\varphi)}]^{T}, \tag{E2}$$

where d is the antenna spacing, and λ is the carrier wavelength.

In simulation, the number of paths follow a random distribution between 1 and 10. The AOD are uniformly distributed in $[30^{\circ},120^{\circ}]$. We adopt the ULAs with antenna spacing $d=\frac{\lambda}{2}$ at APs where $N=4$ and $N_{\mathrm{RF}}=1$. In Fig. 1, the theoretical bound used as a reference is given by

$$R_{\mathrm{UP-Bound}}=\sum_{k=1}^{K}\log_{2}(1+\frac{\hat{\mathbf{H}}_{k}^{\mathrm{H}}\hat{\mathbf{H}}_{k}}{\sigma_{k}^{2}}). \tag{E3}$$

References

1 Chen S, Zhang J, Björnson E, et al. Structured massive access for scalable cell-free massive MIMO systems. IEEE J Sel Areas Commun, 2021, 39: 1086-1100
2 Björnson E, Sanguinetti L. Scalable cell-free massive MIMO systems. IEEE Trans Commun, 2020, 68: 4247–4261
3 Zhao X, Lin T, Zhu Y, et al. Partially-connected hybrid beamforming for spectral efficiency maximization via a weighted MMSE equivalence. IEEE Trans Wireless Commun, 2021, 20: 8218-8232
4 Wu H. Duality theory for optimization problems with interval-valued objective functions. J Optim Theory Appl, 2010, 144: 615–628
5 Yu X, Shen J, Zhang J, et al. Alternating minimization algorithms for hybrid precoding in millimeter wave MIMO systems. IEEE J Sel Topics Signal Process, 2016, 10: 485-500